

# Sharp finite statistics for minimum data block sizes in quantum key distribution

Vaisakh Mannalath<sup>1,2,3,\*</sup>, Víctor Zapatero<sup>1,2,3,\*</sup> and Marcos Curty<sup>1,2,3</sup>

<sup>1</sup>*Vigo Quantum Communication Center, University of Vigo, Vigo E-36310, Spain*

<sup>2</sup>*Escuela de Ingeniería de Telecomunicación, Department of Signal Theory and Communications, University of Vigo, Vigo E-36310, Spain and*

<sup>3</sup>*AtlantTic Research Center, University of Vigo, Vigo E-36310, Spain*

The performance of quantum key distribution (QKD) heavily depends on the finite statistics of its security proof. For multiple protocols and proof techniques, the central statistical task is a random sampling problem, which is customarily addressed by invoking suitable tail bounds on the hypergeometric distribution. In this work, we introduce an alternative solution that exploits a link between random sampling with and without replacement. Despite its simplicity, it notably boosts the achievable secret key rate, particularly in the regime of small data block sizes critical for satellite QKD and other envisioned QKD applications. Moreover, as a by-product of the proposed tool, tight Neyman constructions are derived for the average of independent Bernoulli variables. Bounds of this kind naturally fit in finite-key security proofs of decoy-state QKD schemes, further sharpening the finite statistics compared to previous approaches.

*Introduction.* Quantum key distribution (QKD) is the only approach to key exchange that is provably secure against computationally unbounded adversaries [1]. Today, considerable efforts are being made to boost the performance of practical QKD systems while guaranteeing their physical-layer security [2, 3]. Among the multiple facets of this ongoing program, refining the mathematical security proofs is of utmost importance in order to achieve tighter lower bounds on the extractable secret key length. These security proofs build upon quantum information-theoretic results and rely on statistical prediction and inference. Here, finite statistics play a pivotal role to keep the necessary data block sizes to a minimum. This feature is very desirable for any application of QKD and may be critical for space-to-ground QKD links in low or medium Earth-orbit environments [4–8], where both the raw data collection per satellite overpass and the data storage capacity of the satellite are limited [9–11].

Establishing the finite-key security of a QKD protocol requires to upper bound the probability of a “failure” happening in its parameter estimation (PE) step. This refers to the event where the protocol does not abort but the adversary obtains non-trivial information about the distributed key [1]. In BB84-like protocols [12], a very popular security proof technique is based on the entropic uncertainty relation [13], in which case the simplest formulation of the problem is as follows. Let us consider a two-piece experiment where a population of  $N$  binary random variables (RVs) is generated according to an arbitrary probability distribution, and a random sample of size  $n$  is drawn from the population afterwards. If we denote the frequency of ones in the test (complementary) sample as  $\hat{p}$  ( $\hat{q}$ ), the goal is to find a threshold value

$q^{\text{th}} \geq p^{\text{th}}$  such that

$$\Pr[\hat{p} \leq p^{\text{th}}, \hat{q} \geq q^{\text{th}}] \leq \epsilon, \quad (1)$$

for arbitrary values of  $N$ ,  $n$ ,  $\epsilon$  and  $p^{\text{th}}$ . Naturally, an interplay exists between  $\epsilon$  and  $q^{\text{th}}$ : fulfilling Eq. (1) with a very small  $\epsilon$  comes at the price of tolerating larger values of  $q^{\text{th}}$ . In the context of QKD—in which  $\hat{q}$  is often referred to as the phase-error rate (PHER)—this translates into a direct penalty on the provably secure key length. Remarkably, the above formulation of the problem shows up exactly in ideal implementations of the BB84 [12] or the BBM92 [14, 15] protocols, and we adhere to the latter in the main text for didactic purposes. See Appendix A for the detailed protocol description and secret key length formula. On the other hand, the popular decoy-state BB84 protocol [16–19], which is implemented in most of today’s commercial QKD setups, is addressed in Appendix B.

A threshold value  $q^{\text{th}}$  satisfying Eq. (1) can be obtained from an exponential tail bound on the hypergeometric distribution known as Serfling inequality [20], an approach that is commonplace in QKD security proofs nowadays [15, 21]. Recently, though, a sharper bound has been derived in [22] by suitably splitting the “failure event” into two disjoint scenarios delimited by the total frequency of ones in the population, and finding separate estimates for each of them. In particular, while the first estimate still relies on the original Serfling bound, the second one is based on a refined inequality due to Hush and Scovel [23], resulting in a 14% to 17% reduction of the minimum data block length necessary for the BBM92 scheme with typical channel and protocol settings. Notably though, the improvement reported in [22] with respect to [15] heavily relies on the use of considerably large samples for testing. This is an undesirable feature because the final key is extracted from the complementary data.

In this paper, we propose a fundamentally different approach to calculate  $q^{\text{th}}$ , which exploits a link between

\* These authors contributed equally to this paper.  
vmannalath@vqcc.uvigo.es  
vzapatero@vqcc.uvigo.es

random sampling with and without replacement [24]. Remarkably, the resulting bound outperforms [22] in all the explored parameter regimes relevant for QKD, where one naturally restricts  $p^{\text{th}}$  to a few percent at most,  $N$  and  $n$  to thousands or tens of thousands at least, and  $\epsilon$  to rather minuscule values. In particular, a significant improvement is observed for small data block sizes, where, to the best of our knowledge, [22] provides the tightest analysis in the literature. Precisely, for the BBM92 protocol, we find reductions of the minimum data block length beyond 16% in practically relevant scenarios, while for the decoy-state BB84 scheme we report a reduction of 22% when compared to [22], which is remarkable. Moreover, the advantage becomes larger when considering more demanding (*i.e.* smaller) values of the failure probability  $\epsilon$ . On another note, our bound also surpasses that of [22] in a vast parameter regime alien to QKD, which suggests that it might be of independent interest to other applications.

Furthermore, in the process of deriving the main result, tight analytical Neyman constructions [25] are obtained for the average of independent Bernoulli variables. Importantly, these naturally fit in *e.g.* finite-key security analyses of decoy-state QKD schemes, thereby allowing to further sharpen the finite statistics.

*Technical results.* The key enabler of our method is the elementary observation that tail bounds for binary samples drawn with replacement also hold for samples drawn without replacement, which is a consequence of a more general theorem by Hoeffding [24]. The derivation of the main result involves two conceptual steps. First, Neyman constructions [25] —essentially, confidence intervals— are derived from the additive Chernoff bound [26], a well-known exponential tail bound for sampling with replacement. This step relies on a tight-as-possible rational approximation of the logarithmic function [27] to provide a relaxation of the additive Chernoff bound. Secondly, the upper Neyman construction, which directly extends to the hypergeometric distribution, is recasted in terms of a hypergeometric RV and its complementary RV, and the desired bound follows through an averaging technique similar to those of [15, 21, 22].

First, we provide the statement of the Neyman constructions, a proof of which is given in Appendix C.

**Proposition 1** (Neyman constructions). *Let  $\hat{p}$  be the average of  $n$  independent Bernoulli variables, with expected value  $\mathbb{E}[\hat{p}] = p$ , and let  $\kappa_{n,\epsilon} = (2/9n) \ln(1/\epsilon)$ . Then, for all  $\epsilon > 0$ , we have that  $\Pr[\Gamma_{n,\epsilon}^+(\hat{p}) \leq p] \leq \epsilon$ , where  $\Gamma_{n,\epsilon}^+(x)$  is given by the upper branch of*

$$\Gamma_{n,\epsilon}^{\pm}(x) = \frac{1}{1 + 4\kappa_{n,\epsilon}} \left[ 3\kappa_{n,\epsilon} + (1 - 2\kappa_{n,\epsilon})x \pm 3\sqrt{\kappa_{n,\epsilon}(\kappa_{n,\epsilon} + x - x^2)} \right] \quad (2)$$

for  $x \leq (1 - 2\kappa_{n,\epsilon})/(1 + \kappa_{n,\epsilon})$ , while for  $x > (1 - 2\kappa_{n,\epsilon})/(1 + \kappa_{n,\epsilon})$  the function  $\Gamma_{n,\epsilon}^+(x)$  is extended with the slope at  $x = (1 - 2\kappa_{n,\epsilon})/(1 + \kappa_{n,\epsilon})$ .

Also, for all  $\epsilon > 0$ , we have that  $\Pr[\Gamma_{n,\epsilon}^-(\hat{p}) \geq p] \leq \epsilon$ , where  $\Gamma_{n,\epsilon}^-(x)$  is given by the lower branch of Eq. (2) for  $x \geq 3\kappa_{n,\epsilon}/(1 + \kappa_{n,\epsilon})$ , while for  $x < 3\kappa_{n,\epsilon}/(1 + \kappa_{n,\epsilon})$  the function  $\Gamma_{n,\epsilon}^-(x)$  is extended with the slope at  $x = 3\kappa_{n,\epsilon}/(1 + \kappa_{n,\epsilon})$ .

These constructions automatically extend to a hypergeometric RV because the additive Chernoff bound — from which they are solely derived — also holds in that setting (see Theorem 4 in [24]). Particularly, the extension of the upper Neyman construction is given below.

**Corollary 1.** *Let  $\hat{X} \sim \text{Hypergeometric}(N, K, n)$  and  $\hat{p} = \hat{X}/n$ , such that  $\mathbb{E}[\hat{p}] = p$  with  $p = K/N$ . Then, for all  $\epsilon > 0$ , we have that  $\Pr[\Gamma_{n,\epsilon}^+(\hat{p}) \leq p] \leq \epsilon$ , where  $\Gamma_{n,\epsilon}^+(x)$  is defined in Eq. (2).*

This result readily implies the following proposition.

**Proposition 2** (Random sampling bound). *A test sample of size  $n$  is drawn at random from a binary population with  $N$  elements. Let  $\hat{p}$  ( $\hat{q}$ ) denote the frequency of ones in the test (complementary) sample. For all  $\epsilon > 0$ , we have that*

$$\Pr[\hat{q} \geq q_{N,n,\epsilon}^{\text{th}}(\hat{p})] \leq \epsilon, \quad (3)$$

for

$$q_{N,n,\epsilon}^{\text{th}}(x) = \frac{N\Gamma_{n,\epsilon}^+(x) - nx}{N - n}, \quad (4)$$

where  $\Gamma_{n,\epsilon}^+(x)$  is defined in Eq. (2).

*Proof.* Let  $\hat{X}$  be the number of ones in the test sample, such that  $\hat{p} = \hat{X}/n$ . Since  $\hat{X}$  is hypergeometrically distributed, the claim follows directly from Corollary 1, by substituting  $p = n\hat{p}/N + (N - n)\hat{q}/N$  and rearranging terms.  $\square$

Importantly, as shown next, Proposition 2 allows to obtain a threshold value  $q^{\text{th}}$  fulfilling Eq. (1), thus directly providing the failure probability estimation for the ideal BBM92 protocol.

**Proposition 3** (BBM92 failure probability). *Consider the two-piece experiment presented in the Introduction. Then, for all  $\epsilon > 0$  and  $p^{\text{th}} < 1/2$ , we have that*

$$\Pr[\hat{p} \leq p^{\text{th}}, \hat{q} \geq q_{N,n,\epsilon}^{\text{th}}(p^{\text{th}})] \leq \epsilon, \quad (5)$$

for the function  $q_{N,n,\epsilon}^{\text{th}}(x)$  defined in Eq. (4), given that the latter is locally non-decreasing at  $p^{\text{th}}$ .

*Proof.* Let  $\hat{T}$  denote the frequency of ones occurring in the population. Then,

$$\begin{aligned} \Pr[\hat{p} \leq p^{\text{th}}, \hat{q} \geq q_{N,n,\epsilon}^{\text{th}}(p^{\text{th}})] &\leq \Pr[\hat{q} \geq q_{N,n,\epsilon}^{\text{th}}(\hat{p})] \\ &\leq \sum_p \Pr[\hat{T} = p] \Pr[\hat{q} \geq q_{N,n,\epsilon}^{\text{th}}(\hat{p}) | \hat{T} = p] \leq \epsilon. \end{aligned} \quad (6)$$

In the first inequality we use the fact that  $\{\hat{p} \leq p^{\text{th}}, \hat{q} \geq q_{N,n,\epsilon}^{\text{th}}(p^{\text{th}})\} \implies \{\hat{q} \geq q_{N,n,\epsilon}^{\text{th}}(\hat{p})\}$ . This is so because  $q_{N,n,\epsilon}^{\text{th}}(x)$  is non-decreasing for  $x \in [0, p^{\text{th}}]$  if it is non-decreasing at  $x = p^{\text{th}}$ , and the latter is guaranteed by assumption. The averaging over  $\hat{T}$  in the second inequality is a purely ad hoc step aimed at enabling the use of Proposition 2, which presumes a fixed frequency of ones in the population. The third inequality follows from Proposition 2.  $\square$

A relevant observation is that the condition on the slope at  $p^{\text{th}}$ , which is equivalent to  $\Gamma_{n,\epsilon}^{+\prime}(p^{\text{th}}) \geq n/N$  ( $\Gamma_{n,\epsilon}^{+\prime}(x)$  denoting the derivative of  $\Gamma_{n,\epsilon}^{+}(x)$  with respect to  $x$ ), is unrestrictive for all practical purposes [28]. On another note, we remark that Proposition 2 also provides a building block for the estimation of the failure probability of other QKD schemes; see Appendix B.

In Fig. 1 we compare the threshold values  $q^{\text{th}}$  of Eq. (1) arising from Proposition 3, [22] and [15]. Precisely, we plot  $q^{\text{th}}$  versus  $p^{\text{th}}$  for a range  $p^{\text{th}} \in [0.01, 0.05]$ , setting  $N = 10^6$ ,  $n = N/4$ , and  $\epsilon = 10^{-10}$  for illustration purposes. Notably, the improvement attained by Proposition 3 increases further for lower values of  $p^{\text{th}}$ ,  $n$  and  $\epsilon$ .

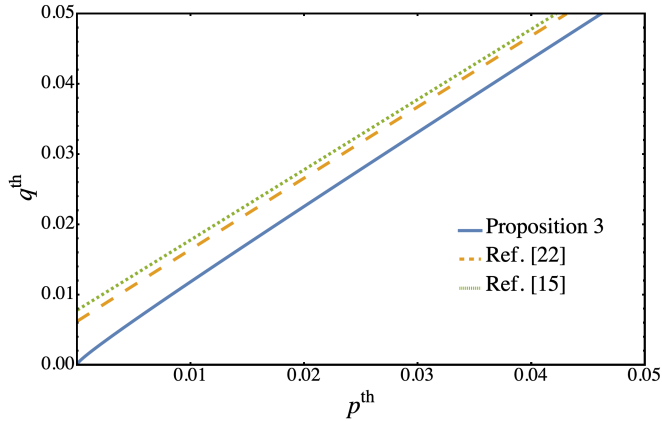


Figure 1: Estimation of  $q^{\text{th}}$  versus  $p^{\text{th}}$  when  $p^{\text{th}} \in [0.01, 0.05]$ ,  $N = 10^6$ ,  $n = N/4$ , and  $\epsilon = 10^{-10}$ . The solid blue line corresponds to Proposition 3 of this work (*i.e.*  $q_{N,n,\epsilon}^{\text{th}}(p^{\text{th}})$ ), while the dashed orange line refers to [22], which combines Serfling [20] and Hush and Scovel [23] inequalities. The dotted green line refers to [15], which is based on Serfling inequality alone.

*QKD simulations.* In what follows, we illustrate the impact that the proposed statistical tools have in the finite-key performance of QKD.

We consider the ideal BBM92 protocol first. Consistently with [15, 22], here we evaluate a simplified scenario in which Alice and Bob share a  $2N$ -partite quantum state as protocol input, and they jointly select between two binary and complementary quantum measurements uniformly at random on a round-by-round basis, in so

each of them extracting a raw data block of  $N$  bits [15]. These blocks are randomly splitted into a fixed-length test (sifted-key) string of  $n$  ( $N - n$ ) bits. That is to say, both the key and the test string are randomly sampled from the two bases.

In the simulations, we set the tolerated quantum bit error rate (QBER) to  $p^{\text{th}} = 4.55\%$  for ease of comparison with [22], where this choice is motivated by the results of the Micius experiment [6]. Also, an error correction (EC) leakage of  $\lambda_{\text{EC}} = 1.19(N - n)h(p^{\text{th}})$  bits is assumed,  $h(x)$  standing for the binary Shannon entropy of  $x$ . The correctness parameter,  $\epsilon_{\text{cor}}$ , and the privacy amplification error,  $\epsilon_{\text{PA}}$ , are both set to  $10^{-8}$  for illustration purposes. On the other hand, the failure probability bound is set to  $\epsilon_{\text{PE}} = 4 \times 10^{-16}$ , which roughly provides the minimum value enabling a low enough  $q^{\text{th}}$  for a nonzero secure key length in the Micius experiment. Altogether, these settings lead to an overall secrecy parameter of  $\epsilon_{\text{sec}} \approx 5 \times 10^{-8}$  (see Appendix A).

With these inputs, in Fig. 2a we plot the extractable secret key length  $l$  divided by the data block size for data blocks ranging from  $N = 2000$  to 8000 bits, showing that our method allows to reduce the minimum block size with respect to [22] in more than 16%. As a side remark, we also note that the approach in [22] would require  $\epsilon_{\text{PE}}$  to be at least  $4 \times 10^{-13}$  to obtain a positive key in the Micius experiment, which is three orders of magnitude larger than what is needed with our tool. In addition, we emphasize that the advantage of our approach increases further if more demanding (*i.e.* smaller) values of  $\epsilon_{\text{cor}}$  and  $\epsilon_{\text{PA}}$  are requested.

Let us now consider the more practical decoy-state BB84 protocol. We assume a scheme with three common intensities per basis,  $\mu$  (signal),  $\nu$  (decoy) and  $\omega$  (vacuum), and deploy the  $Z$  ( $X$ ) basis for key extraction (PE) with a fixed-size data block of  $N_Z$  ( $N_X$ ) bits drawn at random from the corresponding data pool. In the PE step of the protocol, the parties evaluate suitable decoy-state bounds for the single-photon security parameters (*e.g.* the number of single-photon counts and their PHER). If these bounds do not fulfil predetermined acceptance thresholds, the protocol aborts. Otherwise, a fixed-length output key matching the acceptance thresholds is extracted. As explained in Appendix B, the details of the PE test are different depending on the random sampling technique used to bound the PHER.

In the simulations, we consider a range of total data block lengths  $N = N_Z + N_X$  from 3000 to 12000 bits, and take  $N_Z = q_Z^2/(q_Z^2 + q_X^2)N$ , where  $q_Z$  ( $q_X$ ) denotes the probability that each of Alice and Bob selects the  $Z$  ( $X$ ) basis. Also, we set  $\omega = 10^{-4}$  due to the finite extinction ratio of the intensity modulator [29]. The intensities  $\mu$  and  $\nu$ , together with their respective probabilities,  $p_\mu$  and  $p_\nu$ , and the test basis probability,  $q_X$ , are tuned to optimize the secret key rate per block,  $l/N$ . For simplicity, in order to select the acceptance thresholds of the PE tests, the average behaviour of a typical fiber and detector model is considered (see Appendix B for fur-

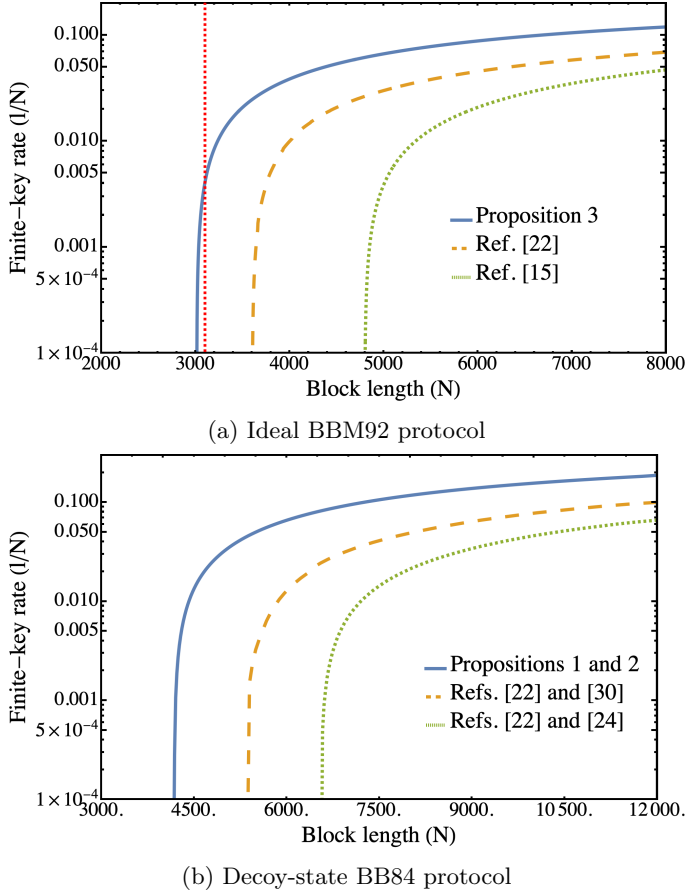


Figure 2: Finite secret key rate per raw data bit as a function of the data block size. (a) Ideal BBM92 protocol. The solid blue line corresponds to Proposition 3 of this work, while the dashed orange (dotted green) line refers to [22] ([15]). The dotted red vertical line indicates the block size gathered in the Micius BBM92 experiment [6], *i.e.*  $N = 3100$  bits. (b) Decoy-state BB84 protocol. The solid blue line corresponds to Propositions 1 and 2 of this work, while the dashed orange (dotted green) line refers to the combination of [22] with [30] ([24]). The experimental parameters considered in the simulations are provided in the text.

ther details). In addition, we assume an overall system loss of 30 dB, a dark count probability of Bob’s detectors of  $p_d = 6 \times 10^{-7}$  [31] and a misalignment error rate of  $e_{\text{mis}} = 5 \times 10^{-3}$  [19]. The EC leakage is set as in the BBM92 protocol, *i.e.*  $\lambda_{\text{EC}} = 1.19N_z h(\theta^{\text{th}})$ . Note, however, that  $\theta^{\text{th}}$  here denotes the correctable QBER of the key block—which is different from the threshold single-photon error rate,  $p^{\text{th}}$ , in the BBM92 scheme—and we set it to the average QBER of the considered channel model for consistency. Lastly, we set again the overall failure probability bound to  $\epsilon_{\text{PE}} = 4 \times 10^{-16}$ , and assume a common value for each individual error term contributing to it [32]. Similarly, we take  $\epsilon_{\text{cor}} = \epsilon_{\text{PA}} = \delta = 10^{-8}$ ,

where  $\delta > 0$  is an intrinsic variable of the security analysis. Overall, this leads to  $\epsilon_{\text{sec}} \approx 2 \times 10^{-7}$ .

The results are shown in Fig. 2b. As seen in the figure, our approach can reduce the minimum block size for key generation by more than 22% compared to previous approaches. The origin of this improvement is twofold: a tighter estimation of the decoy-state bounds (thanks to the use of the Neyman constructions from Proposition 1), and a sharper random sampling bound (provided by Proposition 2).

*Conclusions.* The performance of a QKD system is strongly affected by the finite statistics of its security proof. For instance, in satellite-based QKD, the raw data collection per satellite overpass [6, 9–11] is inevitably restricted, and tight statistical bounds may result in an enormous saving of time and resources. Furthermore, one could envision future QKD applications requiring short keys on-demand for daily transactions with high security standards. For those, a poor statistical analysis could result in an unbearable penalty on the security guarantees.

Here, we have developed two simple analytical tools for the finite statistics of QKD protocols, ultimately relying on the long-known additive Chernoff bound [26]. The first tool is a random sampling bound well-suited for the vast family of security proofs based on the notion of phase-error rate. The second tool, which is a byproduct of the first one, is a pair of Neyman constructions for averages of Bernoulli variables that naturally fit in security proofs of *e.g.* decoy-state QKD protocols [19]. Explicit comparison with prior work shows that our tools provide a neat advantage in many different parameter regimes relevant to QKD, generally downsizing the necessary block sizes for key extraction. In fact, the proposed random sampling bound surpasses existing alternatives [15, 22] in a broad parameter regime alien to QKD as well, which suggests that it might also be of interest to other applications. After all, this bound could in principle be used in disciplines well beyond the realm of QKD, such as quality control tests, clinical trials and hypothesis testing in general.

#### Acknowledgements.

We acknowledge support from the Galician Regional Government (consolidation of Research Units: Atlant-TIC), the Spanish Ministry of Economy and Competitiveness (MINECO), the Fondo Europeo de Desarrollo Regional (FEDER) through the grant No. PID2020-118178RB-C21, MICIN with funding from the European Union NextGenerationEU (PRTR-C17.I1) and the Galician Regional Government with own funding through the “Planes Complementarios de I+D+I con las Comunidades Autónomas” in Quantum Communication, the European Union’s Horizon Europe Framework Programme under the Marie Skłodowska-Curie Grant No. 101072637 (Project QSI) and the project “Quantum Security Networks Partnership” (QSNP, grant agreement No. 101114043). M.C. acknowledges support from a “Salvador de Madariaga” grant from the Spanish Ministry of Science, Innovation and Universities (grant No.



## Appendix A: Ideal BBM92 protocol

### 1. Protocol description

In this section we describe the ideal BBM92 protocol from Ref. [22], where no detection losses are considered and both the key string and the test string are randomly sampled from the two bases. In this scheme, Alice and Bob agree on the protocol inputs specified in Table I, *i.e.* the parameters  $N, n, p^{\text{th}}$ ,  $\lambda_{\text{EC}}$ ,  $\epsilon_{\text{PE}}$ ,  $\epsilon_{\text{cor}}$ , and  $\epsilon_{\text{PA}}$ . Moreover, they share a  $2N$ -partite quantum state and consistently choose between two complementary measurements on a round-by-round basis, sacrificing a random subset of  $n$  measurement outcomes for testing.

The protocol runs as follows:

1. *Measurement*: Alice and Bob measure their quantum states with two complementary measurements, which they select jointly in each round, obtaining a raw data block of size  $N$ . A sifted key string of length  $N - n$  is sampled at random, and the rest of the raw data (*i.e.*  $n$  bits) constitutes the test string.
2. *Parameter estimation* (PE): They publicly reveal the test data and compute the quantum bit error rate (QBER). The protocol is aborted if the QBER exceeds a tolerated threshold value  $p^{\text{th}}$ .
3. *Error correction* (EC): They run a pre-defined EC protocol to reconcile their sifted keys, revealing  $\lambda_{\text{EC}}$  secret key bits at most.
4. *Error verification* (EV): They perform an EV step based on 2-universal hashing, using tags of  $\log(2/\epsilon_{\text{cor}})$  bits at most. If the EV tags do not match, the protocol is aborted. Otherwise, they proceed to privacy amplification.
5. *Privacy amplification* (PA): The parties perform a PA step based on 2-universal hashing, each of them obtaining a final key of length

$$l = \left\lfloor (N - n) \left\{ 1 - h \left[ q_{N,n,\epsilon_{\text{PE}}}^{\text{th}}(p^{\text{th}}) \right] \right\} - \lambda_{\text{EC}} - \log \left( \frac{1}{2\epsilon_{\text{cor}}\epsilon_{\text{PA}}^2} \right) \right\rfloor \quad (\text{A1})$$

bits. Here,  $h(x)$  is the binary Shannon entropy function, while the function  $q_{N,n,\epsilon_{\text{PE}}}^{\text{th}}(x)$  depends on the random sampling tool used for the parameter estimation. These are included in the next section. On the other hand,  $\lambda_{\text{EC}}$  is the EC leakage,  $\epsilon_{\text{cor}}$  is the correctness parameter and  $\epsilon_{\text{PA}}$  is the PA error.

Importantly, this approach yields provably  $(2\sqrt{\epsilon_{\text{PE}}} + \epsilon_{\text{PA}})$ -secret and  $\epsilon_{\text{cor}}$ -correct output keys in virtue of a PA lemma for the smooth min-entropy [33], where  $\epsilon_{\text{PE}}$  denotes the corresponding smoothing parameter. As shown in [15],  $\epsilon_{\text{PE}}$  directly provides an upper bound on the failure probability of the protocol, precisely addressed in the next section.

### 2. Failure probability

We recall that, in the BBM92 protocol above, a PE failure refers to the joint event where the PE test succeeds and the presumed threshold on the phase-error rate (PHER) is incorrect [15, 22]. The threshold  $q_{N,n,\epsilon_{\text{PE}}}^{\text{th}}(p^{\text{th}})$  on the PHER can be tuned to guarantee that the failure probability of the protocol is below  $\epsilon_{\text{PE}}$ . Namely, it can be chosen to enforce  $\Pr[\hat{p} \leq p^{\text{th}}, \hat{q} \geq q_{N,n,\epsilon_{\text{PE}}}^{\text{th}}(p^{\text{th}})] \leq \epsilon_{\text{PE}}$ , where  $\hat{p}$  and  $\hat{q}$  respectively denote the QBER and the PHER. Below we provide suitable candidates for the threshold function based on different statistical tools.

Table I: BBM92 protocol inputs

$N$	Raw data block size
$n$	Test data block size
$p^{\text{th}}$	Threshold value for the QBER
$\lambda_{\text{EC}}$	Error correction leakage
$\epsilon_{\text{PE}}$	Failure probability of the parameter estimation step
$\epsilon_{\text{cor}}$	Failure probability of the error correction step
$\epsilon_{\text{PA}}$	Failure probability of the privacy amplification step

*a. Additive Chernoff bound (this work)*

From Proposition 3 in the main text, we have

$$q_{N,n,\epsilon_{\text{PE}}}^{\text{th}}(p^{\text{th}}) = \frac{N\Gamma_{n,\epsilon_{\text{PE}}}^+(p^{\text{th}}) - np^{\text{th}}}{N - n}, \quad (\text{A2})$$

with  $\Gamma_{n,\epsilon_{\text{PE}}}^+(x)$  given by Eq. (2) of the main text. This corresponds to the solid blue line illustrated in Fig. 2a in the main text.

*b. Serfling and Hush & Scovel inequalities combined [22]*

Using Lemma 1 from [22], a candidate  $q_{N,n,\epsilon_{\text{PE}}}^{\text{th}}(p^{\text{th}})$  is given by the solution to the following minimization problem:

$$\begin{aligned} & \min_{(\xi, q^{\text{th}})} q^{\text{th}}, \\ & \text{such that } q^{\text{th}} - p^{\text{th}} > \xi, \\ & N(p^{\text{th}} + \xi) \in \mathbb{Z}^+, \\ & (N - n)^2 (q^{\text{th}} - p^{\text{th}} - \xi) > 1, \\ & \epsilon_{\text{PE}} = \exp\left(-\frac{2Nn\xi^2}{N - n + 1}\right) + \exp\left\{-2F_{N(p^{\text{th}} + \xi)}\left[(N - n)^2 (q^{\text{th}} - p^{\text{th}} - \xi)^2 - 1\right]\right\}, \end{aligned} \quad (\text{A3})$$

where

$$F_{N(p^{\text{th}} + \xi)} := \frac{1}{N(p^{\text{th}} + \xi) + 1} + \frac{1}{N - N(p^{\text{th}} + \xi) + 1}. \quad (\text{A4})$$

As explained in the Introduction of the main text, this approach provides an optimized combination of Serfling inequality [20] with Hush and Scovel inequality [23]. This corresponds to the dashed orange line plotted in Fig. 2a in the main text.

*c. Serfling inequality [20]*

Using Lemma 6 from [15] (which follows solely from Serfling inequality [20]), we have that

$$q_{N,n,\epsilon_{\text{PE}}}^{\text{th}}(p^{\text{th}}) = p^{\text{th}} + \sqrt{\frac{N(n + 1) \ln(\epsilon_{\text{PE}}^{-1})}{2(N - n)n^2}}. \quad (\text{A5})$$

Indeed, one can easily show that the program of Eq. (A3) can only yield a threshold equal or lower than Eq. (A5). This latter equation corresponds to the dotted green line illustrated in Fig. 2a in the main text.

### 3. Simulations

Here we plot the secret key rate versus the block length for the ideal BBM92 protocol comparing the three methods above. Unlike Fig. 2a in the main text, which only considers block lengths up to 8000, this figure goes up to  $N = 10^6$  bits and shows that the advantage of our method remains even in the large block size regime.

### Appendix B: Decoy-state BB84 protocol

We consider a typical decoy-state BB84 protocol in the lines of [19]. Particularly, three common intensities are used in each basis, and the  $Z$  ( $X$ ) basis is employed for key extraction (PE).

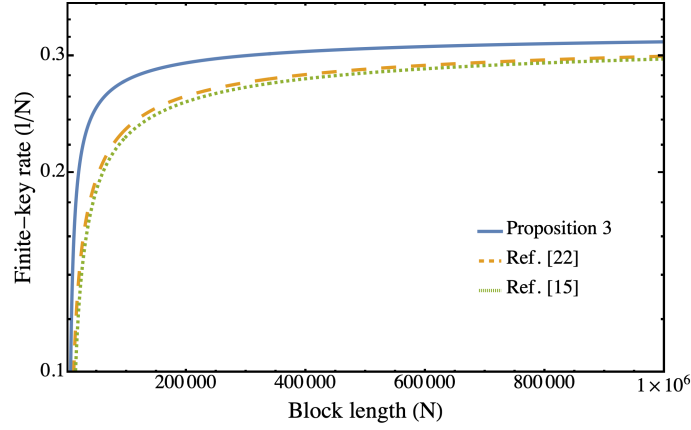


Figure 3: Finite secret key rate per raw data bit as a function of the data block size for the ideal BBM92 protocol with data block sizes up to  $10^6$  bits. The solid blue line corresponds to Proposition 3 of the main text, while the dashed orange (dotted green) line refers to [22] ([15]).

### 1. Protocol description

Alice and Bob agree on the protocol inputs  $T, q_X, \mathcal{K} := \{\mu, \nu, \omega\}, p_\mu, p_\nu, N_X, N_Z, \theta^{\text{th}}, \lambda_{\text{EC}}, \epsilon_{\text{PE}}, \epsilon_{\text{cor}}, \epsilon_{\text{PA}},$  and  $\delta$ , specified in Table II. In addition, if the random sampling tool of Proposition 2 in the main text (or Serfling inequality) is considered, they further agree on two more protocol inputs inherent to the corresponding PE test,  $n_{1,Z}^{\text{th}}$  and  $\phi_{1,Z}^{\text{th}}$ . Alternatively, if the tool of [22] is considered, the additional protocol inputs are  $n_{1,Z}^{\text{th,U(L)}}, n_{1,X}^{\text{th,U(L)}} and  $m_{1,X}^{\text{th,U}}$ , with which they can ultimately define the relevant threshold values entering the secret key length formula:$

$$n_{1,Z}^{\text{th}} = n_{1,Z}^{\text{th,L}}, \quad \phi_{1,Z}^{\text{th}} = \max_{u,v \in \mathcal{B}} q_{u,v,\epsilon_{\text{PE}}}^{\text{th}}(e_{1,X}^{\text{th}}), \quad (\text{B1})$$

where  $e_{1,X}^{\text{th}} = m_{1,X}^{\text{th,U}}/n_{1,X}^{\text{th,L}}$ ,  $\mathcal{B} = \{u \in [n_{1,Z}^{\text{th,L}} + n_{1,X}^{\text{th,L}}, n_{1,Z}^{\text{th,U}} + n_{1,X}^{\text{th,U}}], v \in [n_{1,X}^{\text{th,L}}, n_{1,X}^{\text{th,U}}], u > v\}$ , and the threshold function under consideration is that of Eq. (A3). Importantly, we adopt a more contrived PE test when considering the random sampling tool of [22] in order to simplify the task of bounding the failure probability in Appendix B3b below. Indeed, it is unclear whether a bound can be derived with this tool without modifying the PE test at all. After all, the tool in [22] is devised for the BBM92 protocol specifically, rather than for a decoy-state BB84 protocol, and in this work we provide a possible adaptation to the latter.

The protocol runs as follows. For  $i = 1, \dots, T$ , steps 1 and 2 below are repeated.

1. *State preparation*: Alice chooses a bit value  $y_i$  uniformly at random, a basis setting  $a_i \in \{Z, X\}$  with probability  $q_{a_i}$ , and an intensity setting  $k_i \in \{\mu, \nu, \omega\} =: \mathcal{K}$  with probability  $p_{k_i}$ . She prepares a phase-randomized weak coherent pulse (PRWCP) encoded with the above settings and sends it through the quantum channel to Bob.
2. *Measurement*: Bob measures the incident pulse in the basis  $b_i \in \{Z, X\}$  with probability  $q_{b_i}$ . He records the measurement outcome as  $y'_i \in \{0, 1, \emptyset\}$ , where  $\emptyset$  refers to the “no-click” event. Multiple clicks are assigned to 0 or 1 uniformly at random.

The post-processing and the public discussion run as follows:

3. *Sifting*: The bases and intensity settings are publicly revealed and Alice and Bob identify the sets  $\mathcal{Z} = \{i : a_i = b_i = Z, y'_i \neq \emptyset\}$  and  $\mathcal{X} = \{i : a_i = b_i = X, y'_i \neq \emptyset\}$ .  $N_Z$  rounds are drawn at random from  $\mathcal{Z}$  to form the sifted key data,  $\mathcal{Z}^{\text{sift}}$ , which decomposes as  $\mathcal{Z}^{\text{sift}} = \cup_{k \in \mathcal{K}} \mathcal{Z}_k^{\text{sift}}$  with  $\mathcal{Z}_k^{\text{sift}} = \{i \in \mathcal{Z}^{\text{sift}} : k_i = k\}$  of size  $n_{Z,k}$ .  $N_X$  rounds are drawn at random from  $\mathcal{X}$  to form the test data,  $\mathcal{X}^{\text{test}}$ , which decomposes as  $\mathcal{X}^{\text{test}} = \cup_{k \in \mathcal{K}} \mathcal{X}_k^{\text{test}}$  with  $\mathcal{X}_k^{\text{test}} = \{i \in \mathcal{X}^{\text{test}} : k_i = k\}$  of size  $n_{X,k}$ .
4. *Parameter estimation (PE)*: For each  $k \in \mathcal{K}$ , they disclose the bit values in  $\mathcal{X}_k^{\text{test}}$  and compute the corresponding numbers of bit errors,  $m_{X,k}$ . With the available data, they perform the PE test that matches their preferred random sampling tool (see Appendix B3 for the details). If the test fails, they abort the protocol.

5. *Error correction* (EC): They run a pre-defined EC protocol to reconcile their sifted keys, revealing  $\lambda_{\text{EC}}$  secret key bits at most.
6. *Error verification* (EV): They perform an EV step based on 2-universal hashing, using tags of  $\log(2/\epsilon_{\text{cor}})$  bits at most. If the EV tags do not match, the protocol is aborted. Otherwise, they proceed to privacy amplification.
7. *Privacy amplification* (PA): The parties perform a PA step based on 2-universal hashing, in so obtaining final keys of length

$$l = \left\lfloor n_{1,Z}^{\text{th}} [1 - h(\phi_{1,Z}^{\text{th}})] - \lambda_{\text{EC}} - \log \left( \frac{1}{2\epsilon_{\text{cor}}\epsilon_{\text{PA}}^2\delta} \right) \right\rfloor, \quad (\text{B2})$$

which is provably  $[2(\sqrt{\epsilon_{\text{PE}}} + \delta) + \epsilon_{\text{PA}}]$ -secret and  $\epsilon_{\text{cor}}$ -correct for the requested failure probability bound,  $\epsilon_{\text{PE}}$  [33, 34], carefully addressed in Appendix B 3.

Table II: Decoy-state BB84 protocol inputs alien to the PE test

$T$	Number of transmission rounds
$q_X$	Test basis probability
$\mathcal{K} := \{\mu, \nu, \omega\}$	Set of intensities
$p_\mu$	Probability of setting $\mu$
$p_\nu$	Probability of setting $\nu$
$N_X$	Test data block size
$N_Z$	Key data block size
$\theta^{\text{th}}$	Threshold value for the sifted-key QBER
$\lambda_{\text{EC}}$	Error correction leakage
$\epsilon_{\text{PE}}$	Failure probability of the parameter estimation step
$\epsilon_{\text{cor}}$	Failure probability of the error correction step
$\epsilon_{\text{PA}}$	Failure probability of the privacy amplification error
$\delta$	Slack variable in the entropic chain rule [35]

## 2. Decoy-state analysis

Here, we keep the analytical decoy-state bounds provided in [19] and generalize the statistical analysis, assuming a common error probability  $\varepsilon$  per concentration inequality for simplicity.

The number of single-photon counts in  $\mathcal{Z}^{\text{sift}}$  is lower-bounded as

$$n_{1,Z} \stackrel{3\varepsilon}{\geq} n_{1,Z}^{\text{L}} := \left\lfloor \frac{\tau_1 \mu}{\mu(\nu - \omega) - \nu^2 + \omega^2} \left( \frac{e^\nu}{p_\nu} n_{Z,\nu}^- - \frac{e^\omega}{p_\omega} n_{Z,\omega}^+ - \frac{\nu^2 - \omega^2}{\mu^2} \frac{e^\mu}{p_\mu} n_{Z,\mu}^+ \right) \right\rfloor, \quad (\text{B3})$$

where  $\tau_1 = \sum_{k \in \mathcal{K}} e^{-k} k p_k$ , and the statistical estimates  $n_{Z,k}^\pm$  are given by the functions  $B^\pm(\varepsilon, n_{Z,k}, N_Z)$ , which can be found in Appendix B 2 a to Appendix B 2 c below for the additive and the multiplicative Chernoff bounds [26], and also for Hoeffding inequality [24]. Importantly, the superscript over the inequality symbol in Eq. (B3) indicates that the corresponding bound holds except with probability  $3\varepsilon$  at most. This follows from Boole's inequality [36], noticing that all three statistical estimates have error probability  $\varepsilon$ . We recall that this notation is extensively used below for convenience.

Complementarily to Eq. (B3), it follows that

$$n_{1,Z} \stackrel{2\varepsilon}{\leq} n_{1,Z}^{\text{U}} := \left\lceil \tau_1 \frac{n_{Z,\nu}^+ - n_{Z,\omega}^-}{\nu - \omega} \right\rceil. \quad (\text{B4})$$

Replacing  $Z$  by  $X$  everywhere in Eqs. (B3) and (B4), we reach the corresponding bounds for the single-photon counts in  $\mathcal{X}$ ,  $n_{1,X} \stackrel{3\varepsilon}{\geq} n_{1,X}^{\text{L}}$  and  $n_{1,X} \stackrel{2\varepsilon}{\leq} n_{1,X}^{\text{U}}$ .

The number of bit errors associated with the single-photon events in  $\mathcal{X}$  is upper bounded as,

$$m_{1,X} \stackrel{2\varepsilon}{\leq} m_{1,X}^{\text{U}} := \left\lceil \tau_1 \frac{m_{X,\nu}^+ - m_{X,\omega}^-}{\nu - \omega} \right\rceil, \quad (\text{B5})$$



where  $m_{X,k}^\pm$  are given by the functions  $B^\pm(\varepsilon, m_{X,k}, M_X)$  and  $M_X = \sum_{k \in \mathcal{K}} m_{X,k}$ .

Lastly, it follows that,

$$m_{1,X} \stackrel{3\varepsilon}{\geq} m_{1,X}^L := \left\lfloor \frac{\tau_1 \mu}{\mu(\nu - \omega) - \nu^2 + \omega^2} \left( \frac{e^\nu}{p_\nu} m_{X,\nu}^- - \frac{e^\omega}{p_\omega} m_{X,\omega}^+ - \frac{\nu^2 - \omega^2}{\mu^2} \frac{e^\mu}{p_\mu} m_{X,\mu}^+ \right) \right\rfloor. \quad (\text{B6})$$

Below we briefly review the different candidate definitions we consider for the functions  $B^\pm(x, y, z)$ .

*a. Additive Chernoff bound (this work)*

In the first place, we include the bounds that arise from our Neyman constructions for the additive Chernoff bound [26]. Precisely, it follows from Proposition 1 in the main text that one can take  $B^+(\varepsilon, n\hat{p}, n) := n\Gamma_{n,\varepsilon}^+(\hat{p})$  and  $B^-(\varepsilon, n\hat{p}, n) := n\Gamma_{n,\varepsilon}^-(\hat{p})$ , with the functions  $\Gamma_{n,\varepsilon}^\pm(x)$  given by Eq. (2) in the main text.

*b. Multiplicative Chernoff bound*

Alternatively, one could follow the approach in [30], which is based on the multiplicative form of the Chernoff bound. From [37], we have

$$B^\pm(\varepsilon, n\hat{p}, n) := n\hat{p} \pm \delta^\pm(n\hat{p}, \varepsilon), \quad (\text{B7})$$

for

$$\delta^+(x, y) = x \{W_0[-\exp(-c_{x,y})] + 1\}, \quad (\text{B8})$$

$$\delta^-(x, y) = \begin{cases} -x \{W_{-1}[-\exp(-c_{x,y})] + 1\} & \text{if } x \neq 0, \\ \ln y^{-1} & \text{if } x = 0 \end{cases}, \quad (\text{B9})$$

where  $W_j$  stands for the  $j$ -th branch of the Lambert  $W$  function and  $c_{x,y}$  is defined as  $c_{x,y} = 1 + \ln(1/y)/x$ .

*c. Hoeffding bound*

Lastly, from Hoeffding's inequality [24], we have that

$$B^\pm(\varepsilon, n\hat{p}, n) := n\hat{p} \pm \sqrt{\frac{n}{2} \ln \frac{1}{\varepsilon}}. \quad (\text{B10})$$

### 3. Failure probability

In this section, we bound the failure probability of the decoy-state BB84 protocol for the three random sampling tools under consideration.

*a. Additive Chernoff bound (this work)*

In this case, the PE test is defined by the success event

$$\Omega_{\text{TEST}} = \{n_{1,Z}^L \geq n_{1,Z}^{\text{th}}, \phi_{1,Z}^U \leq \phi_{1,Z}^{\text{th}}\}, \quad (\text{B11})$$

where the threshold values  $n_{1,Z}^{\text{th}}$  and  $\phi_{1,Z}^{\text{th}}$  are the test-specific protocol inputs (see Appendix B 1), the random variable  $n_{1,Z}^L$  is introduced in Appendix B 2, and the random variable  $\phi_{1,Z}^U$  is defined as follows:

$$\phi_{1,Z}^U = \frac{(n_{1,Z}^U + n_{1,X}^U) \Gamma_{n_{1,X}, \varepsilon}^+ \left( \frac{m_{1,X}^U}{n_{1,X}^L} \right) - m_{1,X}^L}{n_{1,Z}^L}, \quad (\text{B12})$$

where the variables  $n_{1,Z}^U$ ,  $n_{1,X}^{L(U)}$  and  $m_{1,X}^{L(U)}$  are also presented in Appendix B 2. Besides, we recall that  $\varepsilon > 0$  is the common error probability settled for each individual concentration inequality in Appendix B 2.

On the other hand, the event where the PE thresholds are not fulfilled by the actual single-photon variables reads

$$\Omega_{\text{PE}} = \{n_{1,Z} \leq n_{1,Z}^{\text{th}}\} \cup \{\phi_{1,Z} \geq \phi_{1,Z}^{\text{th}}\}, \quad (\text{B13})$$

where  $n_{1,Z}$  stands for the number of single-photon counts in the sifted key, and  $\phi_{1,Z}$  stands for the corresponding single-photon PHER.

Given the definitions of  $\Omega_{\text{TEST}}$  and  $\Omega_{\text{PE}}$ , bounding the failure probability of the protocol amounts to finding  $\epsilon_{\text{PE}} > 0$  such that  $\Pr[\Omega_{\text{TEST}}, \Omega_{\text{PE}}] \leq \epsilon_{\text{PE}}$ . This can be easily simplified by noticing that

$$\Pr[\Omega_{\text{TEST}}, \Omega_{\text{PE}}] \leq \Pr[n_{1,Z}^L \geq n_{1,Z} \cup \phi_{1,Z}^U \leq \phi_{1,Z}], \quad (\text{B14})$$

which follows because  $A \implies B$  implies that  $\Pr[A] \leq \Pr[B]$  for arbitrary events  $A$  and  $B$ . Now, it is convenient to introduce the event where all the decoy-state bounds of Appendix B 2 hold. Namely,

$$\Lambda = \{n_{1,Z} \in (n_{1,Z}^L, n_{1,Z}^U), n_{1,X} \in (n_{1,X}^L, n_{1,X}^U), m_{1,X} \in (m_{1,X}^L, m_{1,X}^U)\}. \quad (\text{B15})$$

Making use of  $\Lambda$ , it follows that

$$\Pr[n_{1,Z}^L \geq n_{1,Z} \cup \phi_{1,Z}^U \leq \phi_{1,Z}] \leq \Pr[\bar{\Lambda}] + \Pr[\phi_{1,Z} \geq \phi_{1,Z}^U, \Lambda], \quad (\text{B16})$$

where we simply exploit the fact that  $\Pr[A] \leq \Pr[\bar{B}] + \Pr[A, B]$  (for arbitrary events  $A$  and  $B$ ) and further invoke the trivial implication  $\Lambda \implies n_{1,Z} > n_{1,Z}^L$ . Regarding the first term in the right-hand side of Eq. (B16), carefully counting the errors in Appendix B 2 yields  $\Pr[\bar{\Lambda}] \leq 15\varepsilon$ , and therefore we conclude

$$\Pr[\Omega_{\text{TEST}}, \Omega_{\text{PE}}] \leq 15\varepsilon + \Pr[\phi_{1,Z} \geq \phi_{1,Z}^U, \Lambda]. \quad (\text{B17})$$

All that remains is to set an upper bound on  $\Pr[\phi_{1,Z} \geq \phi_{1,Z}^U, \Lambda]$ . For this, a critical observation is that

$$\Lambda \implies \phi_{1,Z}^U > q_{n_{1,Z} + n_{1,X}, n_{1,X}}^{\text{th}}, \varepsilon \left( \frac{m_{1,X}}{n_{1,X}} \right), \quad (\text{B18})$$

for the threshold function  $q_{N, n, \epsilon_{\text{PE}}}^{\text{th}}(x)$  defined in Eq. (A2). Crucially, note that the right-hand side in the inequality of Eq. (B18) results from “dropping the superscripts” in the left-hand side (given by Eq. (B12)), or equivalently, from replacing the decoy random variables  $n_{1,X(Z)}^{L(U)}$ ,  $n_{1,X(Z)}^{L(U)}$  and  $m_{1,X}^{L(U)}$  by the actual single-photon random variables  $n_{1,X(Z)}$ ,  $n_{1,X(Z)}$  and  $m_{1,X}$ . Indeed, both the definition of  $\phi_{1,Z}^U$  and the choice of  $\Lambda$  are purely ad-hoc in order to enable Eq. (B18), because Proposition 2 in the main text does not apply to the decoy random variables but only to the actual single-photon random variables. In summary, because of Eq. (B18),

$$\Pr[\phi_{1,Z} \geq \phi_{1,Z}^U, \Lambda] \leq \Pr\left[\phi_{1,Z} \geq q_{n_{1,Z} + n_{1,X}, n_{1,X}}^{\text{th}}, \varepsilon \left( \frac{m_{1,X}}{n_{1,X}} \right)\right], \quad (\text{B19})$$

since, again,  $A \implies B$  implies that  $\Pr[A] \leq \Pr[B]$ . At this point, the only technical obstacle for the application of Proposition 2 in the main text is that this bound presumes a population with fixed size and frequency of ones (errors), and also a fixed test sample size. Therefore, by averaging over population sizes,  $n_{1,Z} + n_{1,X}$ , test sample sizes,  $n_{1,X}$ , and total frequencies of errors,  $(m_{1,Z}^{\text{ph}} + m_{1,X})/(n_{1,Z} + n_{1,X})$ —where we have introduced  $m_{1,Z}^{\text{ph}} = \phi_{1,Z} n_{1,Z}$  for clarity—, Proposition 2 in the main text applies for each individual term in the average and, therefore,

$$\Pr\left[\phi_{1,Z} \geq q_{n_{1,Z} + n_{1,X}, n_{1,X}}^{\text{th}}, \varepsilon \left( \frac{m_{1,X}}{n_{1,X}} \right)\right] \leq \varepsilon \quad (\text{B20})$$

follows. Note that this averaging technique is of the exact same nature as the one used to bound the failure probability of the BBM92 protocol (Proposition 3 in the main text), also deployed in [15] and [22]. Lastly, combining this bound with Eqs. (B19) and (B17), we reach  $\Pr[\Omega_{\text{TEST}}, \Omega_{\text{PE}}] \leq 16\varepsilon$ . In conclusion, with the random sampling tool proposed in this work,  $\epsilon_{\text{PE}} = 16\varepsilon$  provides the desired upper bound on the failure probability.

b. *Serfling and Hush & Scovel inequalities combined [22]*

The result in [22] is devised for the ideal BBM92 protocol, and it is a side contribution of this work to make it compatible with the practical decoy-state BB84 protocol. For this purpose, the alternative PE test we consider is

$$\Omega_{\text{TEST}} = \left\{ n_{1,Z}^L \geq n_{1,Z}^{\text{th},L}, n_{1,Z}^U \leq n_{1,Z}^{\text{th},U}, n_{1,X}^L \geq n_{1,X}^{\text{th},L}, n_{1,X}^U \leq n_{1,X}^{\text{th},U}, m_{1,X}^U \leq m_{1,X}^{\text{th},U} \right\}, \quad (\text{B21})$$

where the threshold values  $n_{1,Z}^{\text{th},L(U)}$ ,  $n_{1,Z}^{\text{th},L(U)}$  and  $m_{1,X}^{\text{th},U}$  are the test-specific protocol inputs (see Appendix B1). On the other hand, the event where the PE thresholds do not hold is again given by  $\Omega_{\text{PE}} = \{n_{1,Z} \leq n_{1,Z}^{\text{th}}\} \cup \{\phi_{1,Z} \geq \phi_{1,Z}^{\text{th}}\}$ , recalling that, in this case,  $n_{1,Z}^{\text{th}}$  and  $\phi_{1,Z}^{\text{th}}$  are defined in Eq. (B1) in terms of the thresholds above.

We now introduce the event

$$\Sigma = \{n_{1,Z} \in (n_{1,Z}^L, n_{1,Z}^U), n_{1,X} \in (n_{1,X}^L, n_{1,X}^U), m_{1,X} < m_{1,X}^U\}, \quad (\text{B22})$$

which matches  $\Lambda$  in Eq. (B15) exactly except from the fact that it does not contemplate the condition  $\{m_{1,X} > m_{1,X}^L\}$ . In particular, this implies that  $\Pr[\bar{\Sigma}] = 12\varepsilon$  (composing the relevant errors in Appendix B3), and therefore  $\Pr[\Omega_{\text{TEST}}, \Omega_{\text{PE}}] \leq 12\varepsilon + \Pr[\Omega_{\text{TEST}}, \Omega_{\text{PE}}, \Sigma]$ . Crucially at this point, the ad hoc definitions of  $\Omega_{\text{TEST}}$  and  $\Sigma$  assure the following trivial implications:

$$(\Omega_{\text{TEST}}, \Sigma) \implies \left\{ n_{1,Z(X)} \in (n_{1,Z(X)}^{\text{th},L}, n_{1,Z(X)}^{\text{th},U}), m_{1,X} < m_{1,X}^{\text{th},U} \right\} \implies \left\{ e_{1,X} \leq e_{1,X}^{\text{th}}, \phi_{1,Z}^{\text{th}} \geq q_{n_{1,Z} + n_{1,X}, n_{1,X}, \varepsilon}^{\text{th}}(e_{1,X}^{\text{th}}) \right\}, \quad (\text{B23})$$

where we have introduced the single-photon bit-error rate  $e_{1,X} = m_{1,X}/n_{1,X}$ . Namely, the conjunction of  $\Omega_{\text{TEST}}$  and  $\Sigma$  guarantees that the actual single-photon variables—and not only their decoy-state bounds—fulfil the thresholds of the PE test (first implication in Eq. (B23)), which in turn implies that the random variable  $e_{1,X} = m_{1,X}/n_{1,X}$  is upper-bounded by the value  $e_{1,X}^{\text{th}} = m_{1,X}^{\text{th},U}/n_{1,X}^{\text{th},L}$ , and the value  $\phi_{1,Z}^{\text{th}} = \max_{u,v \in \mathcal{B}} q_{u,v, \varepsilon_{\text{PE}}}^{\text{th}}(e_{1,X}^{\text{th}})$  is equal or larger than the function of random variables  $q_{n_{1,Z} + n_{1,X}, n_{1,X}, \varepsilon}^{\text{th}}(e_{1,X}^{\text{th}})$  (second implication in Eq. (B23)). The latter holds simply because, if the actual single-photon RVs  $n_{1,Z}$  and  $n_{1,X}$  fulfil the thresholds of the PE test, the threshold function evaluated in these variables cannot be larger than the threshold function evaluated in the worst-case variables compatible with the thresholds (captivated by the maximization of some arbitrary inputs  $u$  and  $v$  over  $\mathcal{B}$ ).

In short, we have

$$\begin{aligned} \Pr[\Omega_{\text{TEST}}, \Omega_{\text{PE}}, \Sigma] &\leq \Pr\left[n_{1,Z(X)} \in (n_{1,Z(X)}^{\text{th},L}, n_{1,Z(X)}^{\text{th},U}), m_{1,X} < m_{1,X}^{\text{th},U}, \phi_{1,Z} \geq \phi_{1,Z}^{\text{th}}\right] \\ &\leq \Pr\left[e_{1,X} \leq e_{1,X}^{\text{th}}, \phi_{1,Z}^{\text{th}} \geq q_{n_{1,Z} + n_{1,X}, n_{1,X}, \varepsilon}^{\text{th}}(e_{1,X}^{\text{th}}), \phi_{1,Z} \geq \phi_{1,Z}^{\text{th}}\right] \\ &\leq \Pr\left[e_{1,X} \leq e_{1,X}^{\text{th}}, \phi_{1,Z} \geq q_{n_{1,Z} + n_{1,X}, n_{1,X}, \varepsilon}^{\text{th}}(e_{1,X}^{\text{th}})\right], \end{aligned} \quad (\text{B24})$$

where in the first inequality we invoke the first implication of Eq. (B23)—and disregard the event  $n_{1,Z} \leq n_{1,Z}^{\text{th}}$  of  $\Omega_{\text{PE}}$  because it is incompatible with  $n_{1,Z} \in (n_{1,Z}^{\text{th},L}, n_{1,Z}^{\text{th},U})$ —, in the second inequality we invoke the second implication of Eq. (B23), and in the third inequality we make use of the fact that  $\{\phi_{1,Z}^{\text{th}} \geq q_{n_{1,Z} + n_{1,X}, n_{1,X}, \varepsilon}^{\text{th}}(e_{1,X}^{\text{th}}), \phi_{1,Z} \geq \phi_{1,Z}^{\text{th}}\} \implies \phi_{1,Z} \geq q_{n_{1,Z} + n_{1,X}, n_{1,X}, \varepsilon}^{\text{th}}(e_{1,X}^{\text{th}})$ . To finish with, the desired bound follows from an averaging technique, as usual. Particularly, averaging over population sizes  $(n_{1,Z} + n_{1,X})$  and test sample sizes  $(n_{1,X})$  in this case, it follows that

$$\Pr\left[e_{1,X} \leq e_{1,X}^{\text{th}}, \phi_{1,Z} \geq q_{n_{1,Z} + n_{1,X}, n_{1,X}, \varepsilon}^{\text{th}}(e_{1,X}^{\text{th}})\right] \leq \varepsilon \quad (\text{B25})$$

from the random sampling bound derived in [22]. Putting it all together, we reach  $\Pr[\Omega_{\text{TEST}}, \Omega_{\text{PE}}] \leq 13\varepsilon$ , and thus we can take  $\varepsilon_{\text{PE}} = 13\varepsilon$ .

c. *Serfling inequality* [20]

As mentioned in Appendix B 1, with this tool we define the PE test of the protocol equally as in Appendix B 3 a, but taking

$$\phi_{1,Z}^U = \frac{m_{1,X}^U}{n_{1,X}^L} + \sqrt{\frac{(n_{1,Z}^U + n_{1,X}^U)(n_{1,X}^U + 1) \ln(\varepsilon^{-1})}{2n_{1,Z}^L (n_{1,X}^L)^2}}. \quad (\text{B26})$$

Namely, we use the threshold function of Eq. (A5) rather than that of Eq. (A2). In these circumstances, one can readily prove the failure probability bound  $\epsilon_{\text{PE}} = 13\varepsilon$  reproducing the steps of Appendix B 3 a, but with the ancillary event  $\Sigma$  (Eq. (B22)) rather than  $\Lambda$  (Eq. (B15)). This analogy with Appendix B 3 a comes from the fact that the bound based on Serfling inequality can be stated in the form of Proposition 2 in the main text, just like the bound proposed in this work.

#### 4. Simulations

In this section, we provide some key rate simulations to compare different approaches to the finite statistics of the decoy-state BB84 protocol under consideration. For this, we use a standard channel model of a dedicated fiber [19]. Precisely, the expected detection rate of a signal of intensity  $k$  is given by

$$D_k = 1 - (1 - 2p_d) \exp(-\eta k), \quad (\text{B27})$$

and the probability of having a bit error for intensity  $k$  is given by

$$e_k = p_d + e_{\text{mis}} [1 - \exp(-\eta k)], \quad (\text{B28})$$

where  $p_d$  is the dark count probability of Bob's detectors,  $e_{\text{mis}}$  is the misalignment error rate of the overall system and  $\eta$  is the overall system loss. Namely,  $\eta = 10^{-\lambda/10}$ , with  $\lambda$  denoting the loss in the channel in dB.

This model is used to select the threshold values of the PE test. To be precise, these thresholds are set to the expectation values of the underlying variables according to the channel model. As an example, within the PE test  $\Omega_{\text{TEST}} = \{n_{1,Z}^L \geq n_{1,Z}^{\text{th}}, \phi_{1,Z}^U \leq \phi_{1,Z}^{\text{th}}\}$ ,  $n_{1,Z}^{\text{th}}$  is set to the decoy-state bound of Eq. (B3), upon replacement of  $n_{Z,k}$  by its expectation according to the channel model:

$$\mathbb{E}[n_{Z,k}] = N_Z \frac{p_k D_k}{\sum_j p_j D_j}. \quad (\text{B29})$$

Similarly,  $\phi_{1,Z}^{\text{th}}$  is set to the threshold function derived in this work, upon replacement of all the observables ( $n_{Z,k}$ ,  $n_{X,k}$  and  $m_{X,k}$ ) by their expectations according to the channel model. Particularly,

$$\mathbb{E}[m_{X,k}] = N_X \frac{p_k e_k}{\sum_j p_j D_j}, \quad (\text{B30})$$

and  $\mathbb{E}[n_{X,k}]$  is obtained simply replacing  $Z$  by  $X$  in Eq. (B29).

We remark that the above choices of the thresholds in the PE test are over-optimistic, as they would incur in large abortion probabilities even if the channel behaves according to the considered model. In fact, the ‘‘robustness’’ penalty of using these thresholds is certainly larger when considering the more convoluted PE test devised for the random sampling tool of [22]. This is so because, in that test, double-sided thresholds are imposed, and since both the upper and the lower thresholds are being set to the same value for the simulations, the success probability of the test becomes negligible. In either case, a more sensitive approach consists of making robustness considerations to incorporate statistical fluctuations in the thresholds (ultimately, however, in a real experiment, the thresholds would be chosen via careful channel monitoring).

This said, in Fig. 4 below we plot the secret key rate as a function of the block length  $N = N_Z + N_X$  for the considered decoy-state BB84 protocol. When compared to Fig. 2b of the main text, this figure introduces two additional lines, where we combine the Neyman constructions of Proposition 1 of the main text with either Ref. [22] or [15] for the random sampling bound. These new lines highlight the advantage of our random sampling tool when compared to Ref. [22] or [15] for decoy-state QKD.

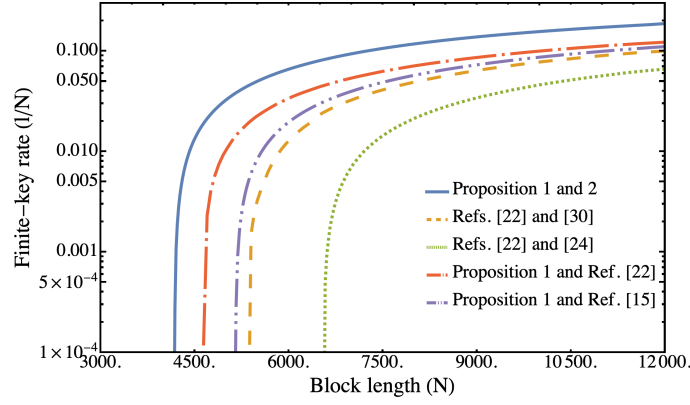


Figure 4: Finite secret key rate per raw data bit as a function of the data block size for the decoy-state BB84 protocol. The solid blue line corresponds to Propositions 1 and 2 of the main text, the dashed orange (dotted green) line combines [22] with [30] ([24]), while the red (purple) line combines Proposition 1 with [22] ([15]). The experimental parameters considered in the simulations are the same as in the main text.

### Appendix C: Neyman constructions for the additive Chernoff bounds

In the first place, we provide a relaxation of the upper additive Chernoff bound [26].

**Proposition 1.** *Let  $\hat{p}$  be the average of  $n$  independent Bernoulli variables, such that  $\mathbb{E}(\hat{p}) = p$ . Then, for all  $z \in [p, 1]$ ,  $\Pr[\hat{p} \geq z] \leq e^{-nD(z,p)}$  for  $D(z,p) = 9(z-p)^2/2(z+2p)(3-z-2p)$ .*

*Proof.* We recall that the original bound [26] is analogous to the above proposition but replacing  $D(z,p)$  by the Kullback-Leibler divergence,

$$D(z||p) = z \ln \left( \frac{z}{p} \right) + (1-z) \ln \left( \frac{1-z}{1-p} \right). \quad (\text{C1})$$

Using the logarithmic inequality  $\ln(1+z) \geq z(6+5z)/2(1+z)(3+z)$  [27] within Eq. (C1) yields  $D(z||p) \geq 9(z-p)^2/(2(z+2p)(3-z-2p)) =: D(z,p)$ . Hence, the desired relaxation follows.  $\square$

Coming next, we reformulate Proposition 1 above to determine the upper bound on  $\hat{p}$  that matches any desired error probability  $\epsilon$ .

**Proposition 2.** *Let  $\hat{p}$  be the average of  $n$  independent Bernoulli variables, such that  $\mathbb{E}(\hat{p}) = p$ . Then, for all  $\epsilon > 0$ ,  $\Pr[\hat{p} \geq z_{n,\epsilon}(p)] \leq \epsilon$  with*

$$z_{n,\epsilon}(p) = \begin{cases} \frac{-b_{n,\epsilon}(p) + \sqrt{b_{n,\epsilon}(p)^2 - 4a_{n,\epsilon}c_{n,\epsilon}(p)}}{2a_{n,\epsilon}} & \text{if } p \leq \frac{1-2\kappa_{n,\epsilon}}{1+4\kappa_{n,\epsilon}}, \\ 1 & \text{otherwise,} \end{cases} \quad (\text{C2})$$

where  $a_{n,\epsilon} = 1 + \kappa_{n,\epsilon}$ ,  $b_{n,\epsilon}(p) = -2p - \kappa_{n,\epsilon}(3-4p)$  and  $c_{n,\epsilon}(p) = p^2 - \kappa_{n,\epsilon}p(6-4p)$  for  $\kappa_{n,\epsilon} = (2/9n) \ln \epsilon^{-1}$ .

*Proof.* According to Proposition 1 above, for all  $z \in [p, 1]$ ,  $\Pr[\hat{p} \geq z] \leq \epsilon$  holds if  $\epsilon = \exp\{-nD(z,p)\}$ . Let us consider the function  $g_{n,p}(z) = \exp\{-nD(z,p)\}$  that maps  $z$ 's to  $\epsilon$ 's for arbitrary  $n$  and  $p$ . Since  $g_{n,p}(z)$  is decreasing and thus injective in  $[p, 1]$ , it is invertible in  $g_{n,p}([p, 1]) = [g_{n,p}(1), 1]$ . Thus, in virtue of Proposition 1, for all  $\epsilon \in [g_{n,p}(1), 1]$   $\Pr[\hat{p} \geq z] \leq \epsilon$  holds if  $z = g_{n,p}^{-1}(\epsilon)$ , which is the only  $z \in [p, 1]$  such that  $g_{n,p}(z) = \epsilon$ . This is a quadratic equation  $a_{n,\epsilon}z^2 + b_{n,\epsilon}(p)z + c_{n,\epsilon}(p) = 0$  with the coefficients prescribed in the statement, and one can readily show that only the larger root, say  $z_{n,\epsilon}^+(p)$ , lies in  $[p, 1]$ . In short,  $\Pr[\hat{p} \geq z_{n,\epsilon}^+(p)] \leq \epsilon$  for all  $\epsilon \geq g_{n,p}(1)$ . Lastly, the claim follows by noticing that  $\epsilon \geq g_{n,p}(1) \Leftrightarrow p \leq (1-2\kappa_{n,\epsilon})/(1+4\kappa_{n,\epsilon})$  and completing the missing range with the trivial bound [38].  $\square$

Proposition 2 above can be used to infer a Neyman [25] construction on the underlying parameter  $p$  in terms of  $\hat{p}$ . For this purpose, we introduce the function  $\tilde{z}_{n,\epsilon}(p)$ , which results from extending  $z_{n,\epsilon}(p)$  with its last slope at the two points where it intersects the  $[0, 1] \times [0, 1]$  square. Precisely, analytical inspection shows that  $z_{n,\epsilon}(p)$  is



monotonically increasing in the interval  $[0, (1 - 2\kappa_{n,\epsilon})/(1 + 4\kappa_{n,\epsilon})]$ , whose extreme points provide the intersections with the  $[0, 1] \times [0, 1]$  square:  $z_{n,\epsilon}(0) = 3\kappa_{n,\epsilon}/(1 + \kappa_{n,\epsilon})$  and  $z_{n,\epsilon}((1 - 2\kappa_{n,\epsilon})/(1 + 4\kappa_{n,\epsilon})) = 1$ . The motivation of “removing the kinks” like this is that Proposition 2 trivially follows as well if we replace  $z_{n,\epsilon}$  by  $\tilde{z}_{n,\epsilon}$ , but  $\tilde{z}_{n,\epsilon}$  has the advantage of being globally invertible, thus enabling the well-definiteness of the random variable  $\Gamma_{n,\epsilon}^-(\hat{p}) = \tilde{z}_{n,\epsilon}^{-1}(\hat{p})$  for all  $\hat{p} \in [0, 1]$ .

**Proposition 3.** *Let  $\hat{p}$  be the average of  $n$  independent Bernoulli variables, such that  $\mathbb{E}(\hat{p}) = p$ . Then, for all  $\epsilon > 0$ ,  $\Pr[\Gamma_{n,\epsilon}^-(\hat{p}) \geq p] \leq \epsilon$  with  $\Gamma_{n,\epsilon}^-(\hat{p}) = \tilde{z}_{n,\epsilon}^{-1}(\hat{p})$ .*

*Proof.* Since  $\tilde{z}_{n,\epsilon}^{-1}$  is monotonically increasing, it follows that  $\{\tilde{z}_{n,\epsilon}^{-1}(\hat{p}) \geq p\} \implies \{\hat{p} \geq \tilde{z}_{n,\epsilon}(p)\}$  irrespectively of  $p$ . Therefore,  $\Pr[\tilde{z}_{n,\epsilon}^{-1}(\hat{p}) \geq p] \leq \Pr[\hat{p} \geq \tilde{z}_{n,\epsilon}(p)] \leq \epsilon$ , where in the last inequality we invoked the relaxation of Proposition 2 above that results from replacing  $z_{n,\epsilon}$  by  $\tilde{z}_{n,\epsilon}$ .  $\square$

Let us now provide an explicit formula for the “principal branch” of  $\Gamma_{n,\epsilon}^-(\hat{p}) = \tilde{z}_{n,\epsilon}^{-1}(\hat{p})$ , corresponding to the interval  $\hat{p} \geq \tilde{z}_{n,\epsilon}(0) = 3\kappa_{n,\epsilon}/(1 + \kappa_{n,\epsilon})$ . Since  $\tilde{z}_{n,\epsilon}^{-1}(\hat{p})$  is the only  $p < \hat{p}$  such that  $\tilde{z}_{n,\epsilon}(p) = \hat{p}$ , solving this quadratic equation for  $p$  (and choosing the relevant root) we conclude that

$$\Gamma_{n,\epsilon}^-(\hat{p}) = \frac{1}{1 + 4\kappa_{n,\epsilon}} \left( 3\kappa_{n,\epsilon} + (1 - 2\kappa_{n,\epsilon})\hat{p} - 3\sqrt{\kappa_{n,\epsilon}(\kappa_{n,\epsilon} + \hat{p} - \hat{p}^2)} \right), \quad (\text{C3})$$

for  $\hat{p} \geq 3\kappa_{n,\epsilon}/(1 + \kappa_{n,\epsilon})$ . For  $\hat{p} < 3\kappa_{n,\epsilon}/(1 + \kappa_{n,\epsilon})$ , the function  $\Gamma_{n,\epsilon}^-(\hat{p})$  is extended with the slope at  $\hat{p} = 3\kappa_{n,\epsilon}/(1 + \kappa_{n,\epsilon})$ . We remark that all the above propositions originate from the upper additive Chernoff bound. Naturally, for each of these propositions, there exists an analogous statement arising from the lower additive Chernoff bound instead. In particular, a Neyman construction complementary to that of Proposition 3 follows.

**Proposition 4.** *Let  $\hat{p}$  be the average of  $n$  independent Bernoulli variables, such that  $\mathbb{E}(\hat{p}) = p$ . Then, for all  $\epsilon > 0$ ,  $\Pr[\Gamma_{n,\epsilon}^+(\hat{p}) \leq p] \leq \epsilon$ , where*

$$\Gamma_{n,\epsilon}^+(\hat{p}) = \frac{1}{1 + 4\kappa_{n,\epsilon}} \left( 3\kappa_{n,\epsilon} + (1 - 2\kappa_{n,\epsilon})\hat{p} + 3\sqrt{\kappa_{n,\epsilon}(\kappa_{n,\epsilon} + \hat{p} - \hat{p}^2)} \right), \quad (\text{C4})$$

for  $\hat{p} \leq (1 - 2\kappa_{n,\epsilon})/(1 + \kappa_{n,\epsilon})$ , and for  $\hat{p} > (1 - 2\kappa_{n,\epsilon})/(1 + \kappa_{n,\epsilon})$   $\Gamma_{n,\epsilon}^+(\hat{p})$  is extended with the slope at  $\hat{p} = (1 - 2\kappa_{n,\epsilon})/(1 + \kappa_{n,\epsilon})$ .

*Proof.* The proof proceeds identically as that of Proposition 3 above, but using the lower additive Chernoff bound as the starting point.  $\square$

Propositions 3 and 4 above correspond to Proposition 1 in the main text.

- 
- [1] Portmann, C. & Renner, R. Security in quantum cryptography. *Reviews of Modern Physics* **94**, 025008 (2022).
  - [2] Xu, F., Ma, X., Zhang, Q., Lo, H.-K. & Pan, J.-W. Secure quantum key distribution with realistic devices. *Reviews of Modern Physics* **92**, 025002 (2020).
  - [3] Lo, H.-K., Curty, M. & Tamaki, K. Secure quantum key distribution. *Nature Photonics* **8**, 595-604 (2014).
  - [4] Liao, S.-K., *et al.* Satellite-to-ground quantum key distribution. *Nature* **549**, 43-47 (2017).
  - [5] Liao, S.-K., *et al.* Satellite-relayed intercontinental quantum network. *Physical Review Letters* **120**, 030501 (2018).
  - [6] Yin, J., *et al.* Entanglement-based secure quantum cryptography over 1,120 kilometres. *Nature* **582**, 501-505 (2020).
  - [7] Chen, Y.-A., *et al.* An integrated space-to-ground quantum communication network over 4,600 kilometres. *Nature* **589**, 214-219 (2021).
  - [8] Cai, W. Q., *et al.* Free-space quantum key distribution during daylight and at night. *Optica* **11**, 647-652 (2024).
  - [9] Bedington, R., Arrazola, J. M. & Ling, A. Progress in satellite quantum key distribution. *npj Quantum Information* **3**, 30 (2017).
  - [10] Sidhu, J. S., Brougham, T., McArthur, D., Pousa, R. G. & Oi, D. K. Finite key effects in satellite quantum key distribution. *npj Quantum Information* **8**, 18 (2022).
  - [11] Roger, T., *et al.* Real-time gigahertz free-space quantum key distribution within an emulated satellite overpass. *Science Advances* **9**, eadj5873 (2023).
  - [12] Bennett, C. H. & Brassard, G. Quantum cryptography: public key distribution and coin tossing. *In Proceedings IEEE International Conference on Computers, Systems & Signal Processing*, 175-179 (IEEE, NY, Bangalore, India, 1984).
  - [13] Tomamichel, M. & Renner, R. Uncertainty relation for smooth entropies. *Physical Review Letters* **106**, 110506 (2011).

- [14] Bennett, C. H., Brassard, G. & Mermin, M. D. Quantum cryptography without Bell's theorem. *Physical Review Letters* **68**, 557 (1992).
- [15] Tomamichel, M. & Leverrier, A. A largely self-contained and complete security proof for quantum key distribution. *Quantum* **1**, 14 (2017).
- [16] Hwang, W. Y. Quantum key distribution with high loss: toward global secure communication. *Physical Review Letters* **91**, 057901 (2003).
- [17] Lo, H.-K., Ma, X. & Chen, K. Decoy state quantum key distribution. *Physical Review Letters* **94**, 230504 (2005).
- [18] Wang, X.-B. Beating the photon-number-splitting attack in practical quantum cryptography. *Physical Review Letters* **94**, 230503 (2005).
- [19] Lim, C. C. W., Curty, M., Walenta, N., Xu, F. & Zbinden, H. Concise security bounds for practical decoy-state quantum key distribution. *Physical Review A* **89**, 022307 (2014).
- [20] Serfling, R. J. Probability inequalities for the sum in sampling without replacement. *The Annals of Statistics* **2**, 39-48 (1974).
- [21] Tomamichel, M., Lim, C. C. W., Gisin, N. & Renner, R. Tight finite-key analysis for quantum cryptography. *Nature Communications* **3**, 1-6 (2012).
- [22] Lim, C. C. W., Xu, F., Pan, J. W., & Ekert, A. Security analysis of quantum key distribution with small block length and its application to quantum space communications. *Physical Review Letters* **126**, 100501 (2021).
- [23] Hush, D., & Scovel, C. Concentration of the hypergeometric distribution. *Statistics & Probability Letters* **75**, 127-132 (2005).
- [24] Hoeffding, W. Probability inequalities for sums of bounded random variables. *Journal of the American Statistical Association* **58**, 13-30 (1963).
- [25] Neyman, J. Outline of a theory of statistical estimation based on the classical theory of probability. *Philosophical Transactions of the Royal Society of London. Series A, Mathematical and Physical Sciences* **236**, 333-380 (1937).
- [26] Chernoff, H. A measure of asymptotic efficiency for tests of a hypothesis based on the sum of observations. *The Annals of Mathematical Statistics* **23**, 493-507 (1952).
- [27] Topsøe, F. Some bounds for the logarithmic function. *Inequality Theory and Applications* **4**, 137 (Nova Publishers, 2007).
- [28] For instance, it is straightforward to show that setting  $\epsilon > \exp\left(-\frac{9(N-n)n}{4(2n+N)}\right)$  suffices to assure that  $\Gamma_{n,\epsilon}^{+'}(p^{\text{th}}) \geq n/N$  for all  $p^{\text{th}} < 1/2$ . This condition on  $\epsilon$  is unrestrictive for all practical purposes.
- [29] Curty, M., Xu, F., Cui, W., Lim, C. C. W., Tamaki, K., Lo, H.-K. Finite-key analysis for measurement-device-independent quantum key distribution. *Nature Communications* **5**, 3732 (2014).
- [30] Zhang, Z., *et al.* Improved key-rate bounds for practical decoy-state quantum-key-distribution systems. *Physical Review A* **95**, 012333 (2017).
- [31] Walenta, N., *et al.* Sine gating detector with simple filtering for low-noise infra-red single photon detection at room temperature. *Journal of Applied Physics* **112**, 063106 (2012).
- [32] The total number of error terms contributing to  $\epsilon_{\text{PE}}$  varies depending on the random sampling tool under consideration, and the reader is referred to Appendix B for the details.
- [33] Tomamichel, M., *et al.* Leftover hashing against quantum side information. *IEEE Transactions on Information Theory* **57**, 5524-5535 (2011).
- [34] Zapatero, V., & Curty, M. Finite-key security of passive quantum key distribution. *Physical Review Applied* **21**, 014018 (2024).
- [35] Vitanov, A., *et al.* Chain rules for smooth min-and max-entropies. *IEEE Transactions on Information Theory* **59**, 2603-2612 (2013).
- [36] Bonferroni, C. Teoria statistica delle classi e calcolo delle probabilita. *Pubblicazioni del R istituto superiore di scienze economiche e commerciali di firenze* **8**, 3-62 (1936).
- [37] Zapatero, V., & Curty, M. Secure quantum key distribution with a subset of malicious devices. *npj Quantum Information*, **7(1)**, 26 (2021).
- [38] Note that the bound becomes identically trivial if  $\kappa_{n,\epsilon} > 1/2$ . Nevertheless, practical situations are typically far away from this very extreme regime.